Confinement and structure of electrostatically coupled dust clouds in a direct current plasma–sheath

S. Nunomura,[a] N. Ohno, and S. Takamura
Department of Energy Engineering and Science, Graduate School of Engineering, Nagoya University, Nagoya 464-8603, Japan

(Received 27 March 1998; accepted 30 June 1998)

Mechanisms for the confinement and the internal structure of an electrostatically coupled dust cloud formed in a dc glow discharge have been investigated from a comparative viewpoint between experimental observations and a simple model. Two kinds of dust clouds with different internal structures are clearly observed, depending on the dispersion of the size distribution of dust particles. The dust cloud can be trapped only in the plasma–sheath boundary area, corresponding to the potential minimum region determined by gravitational and electrostatic forces in the cathode sheath. No dust particles were found deep inside of the sheath, which is consistent with the analysis because the dust particles may be charged positively due to an extreme reduction of the electron density. The internal structure of the electrostatically coupled dust cloud was found to be arranged so that the total potential energy, including the repulsive Coulomb interaction among negative dust particles, may become minimal. © *1998 American Institute of Physics.* [S1070-664X(98)01210-5]

I. INTRODUCTION

Coulomb crystals formed in dusty plasmas have been observed in many capacitively coupled rf devices.[1–5] These crystals are composed of dust particles with almost the same size and may have an ordered internal structure such, as fcc, bcc, or simple hexagonal structure, owing to the repulsive Coulomb interaction among negatively charged dust particles.[6] Such a structural formation was analyzed using a molecular dynamics particle simulation by Totsuji *et al.*,[7,8] in which the system parameters are described to make transitions in the crystal structure. Recently, in several dc glow discharge devices, Coulomb dust clouds have also been found. Fortov *et al.* first observed a Coulomb quasicrystal in the standing striations of a stationary glow discharge, and discussed the factors leading to the formation of a quasicrystal in the striations.[9] Nunomura *et al.* observed a Coulomb dust cloud consisting of vertically heterogeneous layers with different-sized dust particles in the plasma–sheath boundary area.[10] They reported that such a vertical heterogeneous structure is supposed to be formed by the difference in balancing positions between the downward gravitational force and the upward electrostatic one, depending on the different dust size.

In the field of space plasma physics, it is well known that dust particles have been found in many planetary rings, in comets, and on asteroid surfaces,[11,12] whose behavior has a relation to various cosmic phenomena. Heretofore, the behavior of dust particles in a plasma–sheath boundary on asteroidal surfaces has been theoretically investigated by Nitter *et al.*,[13,14] and the mechanisms of charging and trapping of dust particles were discussed there. However, in the case of a dust cloud composed of electrostatically coupled dust particles with negative charge, the confinement and the internal structure has not been examined by quantitatively, comparing experimental observations with an appropriate analysis.

In the present paper, the confinement physics of Coulomb dust clouds formed in the dc plasma–sheath boundary is described with several key points: the charging of dust particles in the sheath and the external potential well structure. The internal structure is discussed in terms of the dispersion of the size distribution of dust particles on the one hand, and the minimization of total potential energy, including the intrinsic repulsive Coulomb interaction, on the other hand.

II. EXPERIMENTAL SETUP

The experiments were performed in a modified dc glow discharge device, which is shown in Fig. 1. Two mesh discharge electrodes with a diameter of 80 mm and a grid wire spacing of 0.28 mm are horizontally placed in the center of the grounded big vacuum chamber to make a plasma. The gap between these electrodes is 20 mm. The dc glow discharge generates an argon plasma around the negatively biased cathode, not only between the discharge electrodes but also above the cathode at a gas pressure of 100–170 mTorr. In a typical operation, the discharge voltage and current are 265–300 V and 0.24–0.54 mA, respectively. The typical plasma parameters measured with a plane Langmuir probe are $T_e \sim 1$ eV and $n_e \sim 1 \times 10^8$ cm^{-3}. At a height of 12 mm from the center of the cathode surface, the biasing ring electrode with the diameter of 40 mm is set to control horizontal confinement of the dust cloud.

The several kinds of spherical dust particles were supplied into the plasma from the dust feeder located above the cathode to investigate the difference in trapping and internal structure of the dust clouds. Part of the dust particles falling into the plasma is trapped in the plasma–sheath boundary area above the center of the cathode while the ring electrode

[a]Electronic mail: s-nunomu@echo.nuee.nagoya-u.ac.jp

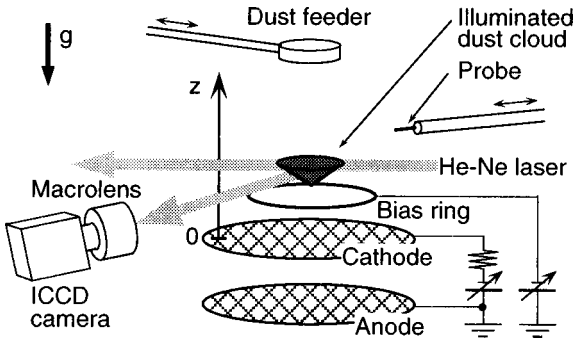

FIG. 1. Schematic view of the experimental apparatus. The argon plasma is produced around the negatively biased cathode by dc glow discharge. The electrostatically coupled dust cloud is trapped at the center of the biasing ring electrode in the plasma–sheath boundary area.

is negatively biased, and form a strongly coupled Coulomb dust cloud in a few seconds. On the other hand, in the case of positive biasing, the dust particles move away horizontally from the center of the ring and are not confined. Clusters composed of many dust particles happen to fall into the plasma from the feeder. However, they are never trapped because of their huge mass. The trapped dust cloud is illuminated by a He–Ne laser light with 632.8 nm in wavelength and 10 mW in output power. The laser light is expanded vertically with a cylindrical lens to catch the hole side view. The thickness and the breadth of the laser sheet are about 700 μm and 20 mm, respectively. The illuminated dust cloud was observed through the side window of the vacuum vessel by using an image-intensified charge-coupled device camera (ICCD camera) with a macrolens of 200 mm. These images are recorded at the rate of 60 frames per second with the shuttering period of 10 ms on a conventional videotape.

III. EXPERIMENTAL RESULTS

Figure 2 shows two different types of dust clouds trapped above the center of the cathode at the same discharge condition. The dust cloud is observed only at the plasma–sheath boundary area, i.e., no dust particles are found deep inside of the sheath. Both clouds have a shape like a three-dimensional funnel with its vertex at the bottom, and their vertical thickness is 1.5–2.5 mm. The shape and internal structure are stable for a long time if the discharge parameters are kept constant, although the dust particles in the clouds are slowly fluctuating around the equilibrium positions, and sometimes exchange those positions for one another. The cloud in Fig. 2(a) is composed of dust particles with the radius of 0.1–1 μm, that is, there is a very large dispersion of the size distribution. The heterogeneous vertical structure of this cloud seems to be made of many horizontal layers, each of which has almost the same sized particles, but the size of particulate becomes large for the deep layers. The mean interparticle distance becomes large when approaching the bottom, where it is about 380 μm. In contrast, the dust cloud shown in Fig. 2(b) consisted of particles with the radius of 1.5 ± 0.25 μm, corresponding to a small dispersion on the size distribution. The dust cloud is constructed by a few horizontal layers periodically located in the

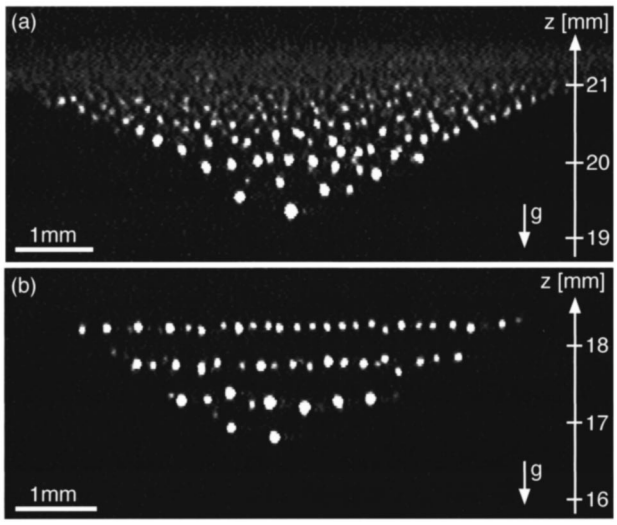

FIG. 2. Two images of typical three-dimensional funnel-shaped dust clouds with (a) the vertically heterogeneous multiple layers and with (b) the superposition of a few discrete horizontal layers. The dust particles with two different dispersions of size distribution are employed to demonstrate the mechanism for the internal structural formation.

vertical direction with a clear finite separation. In each layer, dust particles also seem to be arranged with a regular interval. The mean interparticle distances are about 380 μm in the horizontal and 490 μm in the vertical directions, respectively. Furthermore, by carefully looking at the image it seems to us that the interparticle distances in the upper planes are smaller than those in the lower ones, and the large particles in the distribution levitated in the lower planes, which can be seen in the image due to their greater brightness. It is thought that the large particles acquire large negative charges, and the Debye length in the lower area of the cloud is larger due to the reduction of the shielding ion density, so that the interparticle distances become larger. Such a discrete layered structure is quite different from the above-mentioned heterogeneous dust cloud. Careful observation of these two structures reveals that the internal structure depends critically on the dispersion of the size distribution of the dust particles. Therefore, we can say that the dust cloud is constructed with a more ordered internal structure with a smaller dispersion of the size distribution.

The Coulomb coupling parameter Γ is determined by the ratio of the Coulomb potential energy to the thermal energy of particles.[15,16] It is a measure of electrostatically coupling strength of such a plasma. Here Γ is represented by

$$\Gamma = \frac{Q_d^2}{4\pi\epsilon_0 d \cdot k_B T_d} \exp\left(-\frac{d}{\lambda_D}\right), \tag{1}$$

where Q_d is the charge on a dust particle, d is the mean interparticle distance, and T_d is the temperature for thermal motion of dust particles. In the above-mentioned plasma parameters, the Debye length λ_D is estimated to be 240–530 μm, with the assumption of ion temperature of 0.1–0.5 eV, and the charge on a dust particle with micrometer size is inferred to be thousands of electrons, which is described in the next section. So, Γ is calculated to be 10–380 for the

heterogeneous dust cloud, and 120–780 for the latter ordered cloud, by assuming $T_d \sim 300$ K, respectively. These values indicate that dust particles in both clouds are strongly coupled through the repulsive Coulomb interaction to each other.

IV. SPACE POTENTIAL PROFILE IN THE CATHODE SHEATH

In order to make clear the mechanism of the confinement and the internal structure of the observed dust clouds, it is necessary to estimate the space potential profile and the charges on each dust particle in the sheath formed in front of the cathode surface. The profile of space potential in the sheath is generally inferred from the behavior of ions flowing from the plasma. At a high gas pressure, as mentioned in the previous section, the ions accelerated by a downward electric field in the sheath collide frequently with gas molecules. The equation of motion for ion fluid is expressed as follows:

$$n_i m_i \frac{d\nu_{id}}{dt} = n_i e E_s - \frac{n_i m_i \nu_{id}}{\tau_{i-n}}, \tag{2}$$

where ν_{id} is the mean velocity for drifting ions induced by the electrostatic field in the sheath, τ_{i-n} is the collision time for drifted ions with molecules and E_s is the downward electrostatic field in the sheath. In a steady state, the relation between the ion drift velocity and the electrostatic field is represented by

$$eE_s = \frac{m_i \nu_{id}}{\tau_{i-n}}. \tag{3}$$

Here, the ion–molecule collision time is given by $\tau_{i-n} = \lambda_{i-n}/\nu_{id}$ when the drifted ion velocity is much larger than the ion thermal velocity, so that the ion drift velocity is derived to be

$$\nu_{id} = \sqrt{\frac{e\lambda_{i-n}E_s}{m_i}} = \mu_i E_s^{1/2}, \tag{4}$$

where λ_{i-n} is the mean-free path for drifted ions colliding with molecules and μ_i is given by $(e\lambda_{i-n}/m_i)^{1/2}$. As the recombination and the ionization are neglected in the sheath, the ion flux streaming from the plasma toward the negatively biased cathode surface is conserved so that the ion density is given by the following continuity equation:

$$n_i \nu_{id} = n_{se} C_s, \tag{5}$$

where n_{se} and C_s are the plasma density and the drifted ion velocity at the sheath edge, respectively. The ion flow velocity at the sheath edge is assumed to be the ion sound velocity C_s.[17] The electrostatic potential V_s in the cathode sheath is given by ionic space charge though the Poisson equation:

$$\nabla^2 V_s = -\frac{e(n_i - n_e)}{\epsilon_0} \sim -\frac{en_i}{\epsilon_0}. \tag{6}$$

The electron density is generally much less than the ion density in the sheath due to a large negative potential against the penetration of plasma electrons, so we can neglect it. The substitution of Eqs. (4) and (5) into Eq. (6) gives the distribution of space potential with respect to the bulk plasma potential as follows:[10,18]

$$V_s = -\frac{3}{5}\left(\frac{3}{2}\frac{en_{se}C_s}{\epsilon_0 \mu_i}\right)^{2/3}(\delta - z)^{5/3}, \tag{7}$$

where δ is the thickness of the cathode sheath and z is the height from the cathode surface. From substituting the previously mentioned plasma parameter and the discharge voltage of 290 V into Eq. (7), δ is estimated to be about 26 mm, which agrees well with the experimentally observed thickness of the dark space on the cathode.

V. CHARGING ON A DUST PARTICLE

The charge Q_d on a dust particle in the plasma–sheath is generally given by the product of the capacitance C_d and the floating voltage V_f of the dust particle, i.e., $Q_d = C_d \cdot V_f$. For a spherical dust with the radius of r_d, C_d is obtained to be $4\pi\epsilon_0 r_d$ so that the typical charge on a dust particle with $r_d = 1\ \mu$m may be an order of thousands of elementary electric charge for a few eV in V_f. The floating voltage is generally determined by the balance between the electron and the ion current flowing into the surface of a dust particle. Here, V_f is defined as the potential difference between the surface of the dust particle and the space around the dust. The electron current into a spherical dust is given for the Maxwell–Boltzmann distribution by[19]

$$I_e = -4\pi r_d^2 e \frac{n_e}{4}\left(\frac{8k_B T_e}{\pi m_e}\right)^{1/2} \exp\left(\frac{e(V_s + V_f)}{k_B T_e}\right), \tag{8}$$

where the density reduction of electrons due to the potential drop in the sheath is included. The ion current into a dust is described by[19]

$$I_i = \pi r_d^2 e n_i \left(\frac{k_B T_e}{m_i}\right)^{1/2}\left(1 - \frac{2eV_f}{k_B T_i + m_i \nu_{id}^2}\right), \tag{9}$$

which includes the collection of ions due to the orbit modification by the Coulomb collision with a negatively charged dust particle. In the equilibrium, the floating voltage should be given for these two currents to balance, i.e., $I_e + I_i = 0$. In the case of $n_e = n_i$, that is, the dust density is much smaller than n_e, V_f is eventually represented to satisfy the following equation:[20]

$$\left(\frac{8k_B T_e}{\pi m_e}\right)^{1/2} \exp\left(\frac{e(V_s + V_f)}{k_B T_e}\right) = \left(\frac{k_B T_e}{m_i}\right)^{1/2}\left(1 - \frac{2eV_f}{k_B T_i + m_i \nu_{id}^2}\right). \tag{10}$$

The space potential profile and floating voltage of the dust particle near the cathode sheath edge are shown in Fig. 3 under the experimental condition, in which V_f is numerically obtained. The space potential decreases gradually at the sheath edge and is sharply dropped in the deep inside. The dust particle is charged up negatively only in the plasma–sheath boundary area. Interestingly, the floating voltage approaches zero in a little bit inside of the sheath, and becomes positive in the deep area because of an extreme reduction of

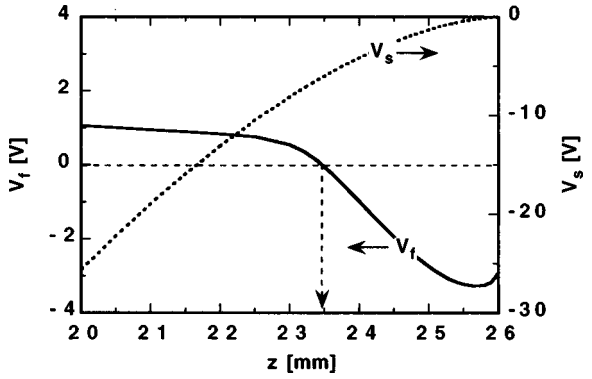

FIG. 3. Space potential V_s (broken line) in the cathode sheath with respect to the plasma potential, and the floating potential V_f (solid line) of a dust particle with respect to the local space potential. The polarity of V_f changes at a little bit inside of sheath, and V_f becomes positive in the deep inside of sheath.

the electron density due to the high potential barrier for plasma electrons. The fact that the charge polarity of a dust particle changes in the sheath is quite important for the levitation depth of the dust cloud, which is described in detail in the next section.

VI. CONFINEMENT FOR DUST PARTICLES

In the dc plasma–sheath without a magnetic field, various forces are at work on dust particles, such as the gravitation, the external electrostatic force, the repulsive Coulomb force among dust particles, and the friction force with ions and molecules.[21] For the horizontal trapping, we consider that the dust cloud is radially confined by the inward electrostatic force based on the outward electrostatic field induced by the ring biasing electrode. It is considered that the inward electrostatic force is larger than the repulsive Coulomb force among dust particles. We assume that the attractive force among negatively charged dust particles, supposed to be generated by the compensation of positive ions immersing them, could be negligibly small.

For the vertical levitation of the dust cloud, we suppose that the upward electrostatic force F_E based on the external electrostatic field in the sheath suspends negatively charged dust particles against the downward gravitational force F_g. The other forces working on a dust particle with $r_d \sim 1\ \mu$m are estimated to be smaller than these two forces by an order of magnitude. The equilibrium condition between both forces, $F_g = F_E$, gives the relation between the radius of a dust particle and the balancing position as follows:[10,13,14]

$$r_d = \left(\frac{3\epsilon_0 V_f}{\rho g}\right)^{1/2} \left(\frac{3}{2}\frac{e n_{se} C_s}{\epsilon_0 \mu_i}\right)^{1/3} (\delta - z)^{1/3}, \tag{11}$$

where ρ is the mass density for the material of dust particles. Figure 4(a) shows the relation between size of a dust particle and the equilibrium height. We find that an upper size limit of the dust particles that can be levitated is $r_d \sim 2.7\ \mu$m. In the deep inside area of the sheath, there is no equilibrium point, in spite of the presence of the large electrostatic field, because the dust particle has a positive charge there, as shown in Fig. 3. Thereby, we can say that dust particles are

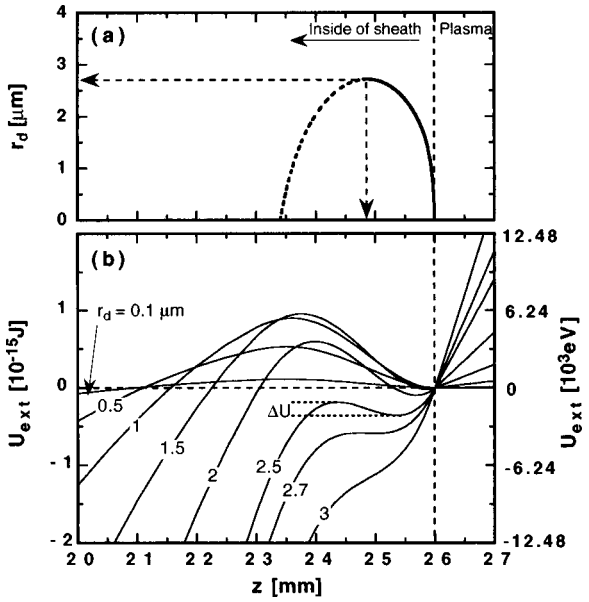

FIG. 4. The equilibrium position of dust particles between the downward gravitational force and the upward electrostatic force in (a), and the profile of potential energy W_{ext} for a single dust particle coming from the gravitational and the upward electrostatic forces in the sheath, as shown in (b). The unstable equilibrium position is shown as a broken line in (a) corresponding to the maximum point for the potential curve in (b). The potential energy is calculated with respect to that at the sheath edge.

not supported against gravitational force deep inside the sheath because of the downward electrostatic force on a dust particle. On the contrary, there are two equilibrium points for a dust particle near the sheath edge. The dust particle located at the lower equilibrium point has a smaller negative charge in the larger electric field, in comparison with that at the higher equilibrium point. To specify whether these two equilibrium points are stable or not, the potential energy U_{ext} profiles for a single dust particle due to the gravitational and the electrostatic forces are plotted in Fig. 4(b), taking the radius of the dust sphere as a parameter. It is quite obvious that the equilibrium point located on the lower side of the sheath is found to be unstable, corresponding to the maximum of the potential energy distribution, and another equilibrium point in the plasma facing side is stable due to the potential well.

In addition, the potential energy curves gives us the barrier energy of a confined dust particle. The barrier energy ΔU determined by the energy difference between the maximum and the minimum is shown in Fig. 5 as a function of the dust radius. It indicates that ΔU becomes maximum at $r_d \sim 1.5\ \mu$m. The barrier energy is an order of 10^{-16} J in a range of $r_d = 0.1$–$1.7\ \mu$m, that is, ΔU corresponds to the potential barrier of a few volts for a dust particle with several thousands of electrons. Therefore, the potential barrier energy is much larger than the thermal kinetic energy of dust particles at room temperature by four orders of magnitude, so that dust particles are thought to be well confined at the potential minimum. The dust particle with large barrier energy is robust for confinement against electrostatic fluctuation in the discharge and the thermal motion of dust particles. Consequently, dust particles are only confined in the

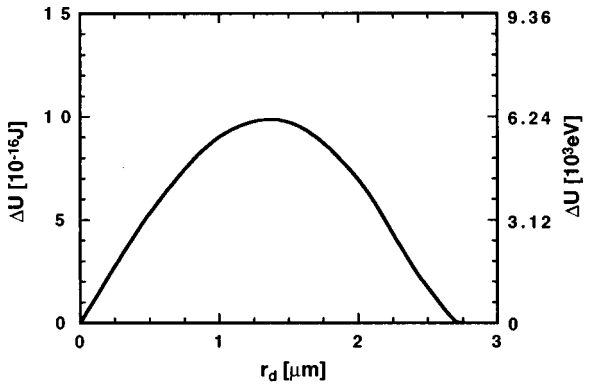

FIG. 5. The potential barrier energy for dust particles as a function of dust size. The dust particle with $r_d \sim 1.5\ \mu$m may have maximum barrier potential energy. The vertical axis on the right hand indicates the energy units in eV.

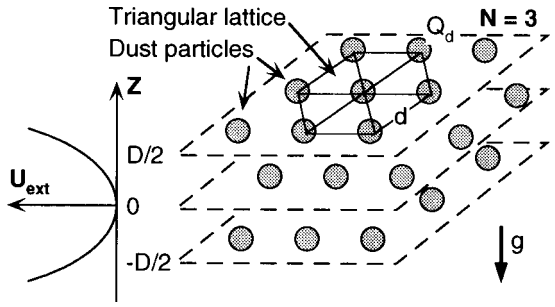

FIG. 6. Model for the electrostatically coupled dust cloud, which is assumed to be made of discrete layers with the regular interval in the vertical direction. Negatively charged dust particles are arranged in a triangular lattice on the layer.

plasma–sheath boundary area, that is, in the potential well made from the upward electrostatic and downward gravitational forces, which agrees with the levitation area of observed dust clouds.

For the behavior of a trapped dust particle in the potential well, the potential curve also implies that the dust particle may vibrate vertically around the potential minimum with the eigenfrequency given by the potential distribution.[13,14] If the displacement of a dust particle at the equilibrium point is small enough, that is, the energy for the eigenoscillation is smaller than the potential barrier energy, we can assume the potential well curve as a parabolic function: $U_{\rm ext}=kz^2/2$. Hence, the eigenfrequency f is expressed as follows:

$$f=\frac{1}{2\pi}\sqrt{\frac{k}{m_d}}, \tag{12}$$

where k is the coefficient describing the potential well curve shown in Fig 4(b). The typical value of k is about 1×10^{-10} N/m for the charged dust particle, with $r_d \sim 1.5\ \mu$m under our experimental condition. Then, the eigenfrequency is estimated to be around 10 Hz. It is thought that this simple calculation is overestimated in comparison with the real eigenfrequency, because we are not taking the friction with plasma particles and molecules into account in the above expression. In the high gas pressure, we suppose that dust particles vibrate more slowly at the potential minimum.

VII. INTERNAL STRUCTURE OF DUST CLOUD AND DISCUSSION

In this section, we discuss the mechanism for the internal structural formation of the observed dust clouds in comparison with a simple analytical model. For the heterogeneous layered structure of the dust cloud shown in Fig. 2(a), the key point is that the balancing position and the charge of each dust particle depend on the particle size. The stable equilibrium positions balancing the electrostatic upward force with the gravitational downward force are distributed over the sheath edge shown in Fig. 4(a), in which a large dust particle is balanced at a lower part of the sheath. Therefore, it is thought that the heterogeneous structure can be explained mainly by the difference of stable equilibrium positions of dust particles distributed over the plasma–sheath boundary area according to the size distribution. Consequently, the heavier and larger dust particles are located at the lower part of the sheath to obtain the larger upward electrostatic force. In addition, this interparticle distance is larger than the one between the small particles located in the upper part of the sheath because large particles acquire large negative charges depending on the dust size, and the Debye length in the lower area of the cloud is larger due to the reduction of the shielding ion density.

On the contrary, in the case of discrete layered structure composed of particles with the small dispersion, the abovementioned argument is not enough to explain the physical mechanism of its internal structural formation. The force balance analysis for the dust cloud with monodisperse particles predicts a monolayered structure, since there is only one stable equilibrium position in the sheath. In fact, it seems to us that the dust cloud tends to expand its structure vertically by repulsive Coulomb interaction among dust particles, since the dust cloud is radially pushed inward by the electrostatic field induced by the negatively biased ring electrode. In order to explain the observed Coulomb dust cloud with a discrete layered structure, we should take the potential energy coming from the repulsive Coulomb force into account. We consider the internal force of the dust cloud with discrete layered structure as modeled in Fig. 6, in which the dust cloud is assumed to be composed of infinite parallel layers with a constant separation in the vertical direction. The model considers the layer composed of a triangular lattice with negatively charged dust particles at its lattice point. In such a model, the total potential energy of the dust cloud is given by the sum of potential energies coming from the gravitational force, electrostatic force in the sheath, and the repulsive Coulomb force among negatively charged particles.[9] The potential energy of a single particle for a gravitational and electrostatic force has already been given, as shown in Fig. 4(b). To simplify the calculations, we approximate the potential well curve for confinement as a parabolic function again. Then, its potential energy $W_{\rm ext}$ for the cloud with the layer number of N per unit area is expressed by

$$W_{\text{ext}}=\sum_{i}^{N} \frac{kz_i^2}{2}\frac{\sigma}{N}, \tag{13}$$

where z_i is the height of each layer and σ is the dust particle density per unit area. We note that W_{ext} becomes zero for the monolayered dust cloud, and it becomes large for a thick dust cloud with a small number of layers if keeping σ constant.

For the Coulomb coupling energy among particles, we consider both energy coming from the force between discrete layers and the one among dust particles on the same layer with a triangular lattice. The shielded Coulomb potential energy $W_{\text{C layer}}$ between different layers per unit area is given by (see the Appendix)

$$W_{\text{C layer}}=\sum_{i,}\sum_{j;i\neq j}\frac{\lambda_{\text{D}}\sigma^2 Q_d^2}{4\epsilon_0 N^2}\exp\left(-\frac{z_{ij}}{\lambda_{\text{D}}}\right), \tag{14}$$

where the summation is carried out for all layers. Here $W_{\text{C layer}}$ also becomes zero in the case of a monolayer, and it tends to become large for a thin dust cloud with many layers at constant σ because the interlayer space becomes narrow. The repulsive Coulomb potential energy $W_{\text{C lattice}}$ among negatively charged dust particles on the same layer per unit area is given by

$$W_{\text{C lattice}}=\sum_{j,i\neq j}^{\text{in layer}}\frac{\sigma Q_d^2}{8\pi\epsilon_0 r_{ij}}\exp\left(-\frac{r_{ij}}{\lambda_{\text{D}}}\right), \tag{15}$$

where r_{ij} is the distance between two dust particles on the same layer, and the summation is carried out for all dust particles on the horizontal layer. Equation (15) indicates that $W_{\text{C lattice}}$ becomes large when the number of layers decreases as σ is kept constant because the interparticle distance becomes small.

Eventually, the total potential energy W_{tot} is given by

$$W_{\text{tot}}=W_{\text{ext}}+W_{\text{C layer}}+W_{\text{C lattice}}. \tag{16}$$

Figure 7(a) shows the contour plots of total potential energy of the dust cloud, including the shielded repulsive Coulomb interaction in the parameter space of layer number N and thickness D of the cloud. The numerical analysis is carried out under the following conditions: $\lambda_{\text{D}}=530\ \mu\text{m}$, $Q_d=4000e$, $\sigma=4\times10^7\ \text{m}^{-2}$, and $k=1\times10^{-10}$ N/m. We distinguish a minimum point in the parameter space, corresponding to six layers with a thickness of about 2 mm. Such an internal structure given by the present simple analysis is consistent with that of the observed dust cloud. The slice distributions for the components of the total potential energy: W_{ext}, $W_{\text{C layer}}$, $W_{\text{C lattice}}$, and W_{tot} on the horizontal lines with $D=2$ mm and the vertical line with $N=6$ are shown in Figs. 7(b) and 7(c), respectively. It indicates that the Coulomb energy between layers has about half of the total potential energy near the minimum point, and two other components, i.e., W_{ext} and $W_{\text{C lattice}}$, share another half of the total. In relation to the transition in the layer number of the cloud, we note that the Coulomb interaction between layers becomes strong when the layer number increases. On the other hand, the Coulomb interaction among particles becomes dominating when the layer number decreases. Furthermore, concerning the change in the cloud thickness, we note that the Coulomb interaction energy between layers becomes large with a decrease in cloud thickness, and the potential energy for vertical confinement increases for the thick cloud. Therefore, we can conclude that the electrostatically coupled dust cloud is self-organized so that a total potential energy including repulsive Coulomb interactions among dust particles may have a minimum.

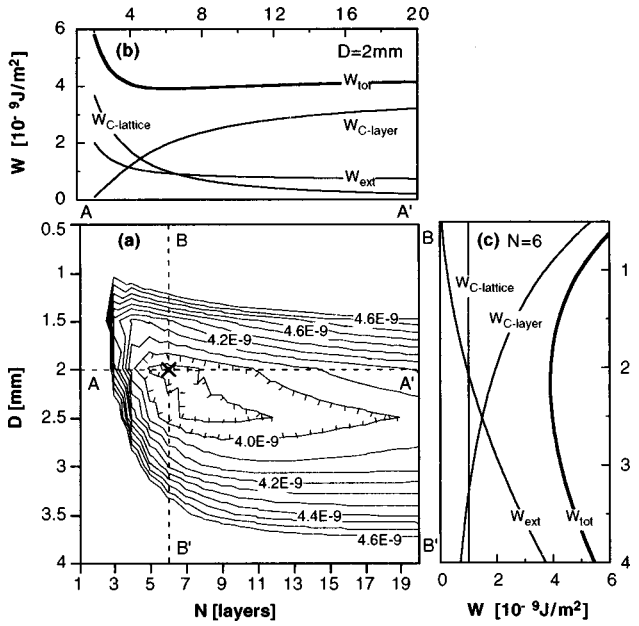

FIG. 7. Contour plots (a) of the total potential energy of the dust cloud, including the shielded Coulomb interaction among particles in parameter space of the thickness D and the layer number N of the cloud. Numerical figures on the contours represent the potential energy with units of J/m^2. The slice distributions of the total potential energy on the broken lines through $A-A'$ ($D=2$) and $B-B'$ ($N=6$) are plotted in (b) and (c), respectively, together with several components of one. The cloud with $D\sim2$ mm and $N=6$ has a minimum of total potential energy under the present experimental condition.

In order to discuss the stability for such a multilayered structure, it is necessary to take the self-gravity effect on a whole dust cloud into account.[22] The self-gravity produces a vertical pressure on a strongly coupled dust cloud so that we suppose that the trapping height is pushed down. The stable structure might be destroyed by this effect, especially around the bottom of the cloud. Then, we evaluate the stability of the internal structure from a comparative viewpoint between the transition energy and the thermal kinetic energy. The thermal kinetic energy W_{thermal} for the dust cloud with the temperature of T_d per unit area is represented by

$$W_{\text{thermal}}=\tfrac{3}{2}\sigma k_{\text{B}}T_d. \tag{17}$$

For the dust cloud with $T_d=300$ K, the thermal kinetic energy is about 2.5×10^{-13} J/m^{-2}. For example, the transition energy of the dust cloud with $D=2$ mm for the layer number from $N=6$ to $N=5$ or 7 is $1.1-1.4\times10^{-11}$ J/m^2, and it corresponds to 44–56 times as large as the thermal energy. Therefore, we concluded that the transition in structure induced by thermal motion of dust particles at room temperature would be quite difficult, so that it is reasonably consis-

tent with our experimental observation, that is, the internal structure of the dust cloud with discrete layers is stably maintained for a long time.

Finally, the mechanism for the formation of the funnel-shaped structure of dust clouds is not clear at the moment. In order to explain such an interesting structure, the above-mentioned simple argument is not sufficient, namely, we should take account of other factors, for example, the effect of the radial electrostatic field with a certain vertical dependence near the sheath edge and the space-charge compensation by the ion fluid immersing between negatively charged dust particles. This subject remains to be clarified in the future.

VIII. CONCLUSION

The mechanisms of the confinement and the internal structure of an electrostatically coupled dust cloud are investigated from the comparison of the experiment with the simple numerical modeling. In the dc plasma–sheath, we identified an upper limit of dust size for the dust suspension. The dust particles are trapped at one of two equilibrium positions and are stable due to the robust potential well. The other equilibrium position at deep inside the sheath is unstable due to the potential maximum. The dispersion of the size distribution of the dust particles drastically changes the internal structure of the electrostatically coupled cloud. The overall Coulomb coupling energy influences the structural formation so much that the discrete layers are formed to minimize the total potential energy, including the internal Coulomb interaction among charged particles in the dust cloud with a small dispersion of the size distribution.

ACKNOWLEDGMENTS

One of the authors (S.N.) would like to thank Dr. Y. Uesugi (Nagoya University), T. Misawa and K. Asano for their many useful discussions, and M. Takagi (Nagoya University) for his technical help.

This work was supported in part by a Grant-in-Aid for Scientific Research from the Japan Ministry of Education, Science, Sport, and Culture (JSPS Research Fellow, No. 3254).

APPENDIX: THE DERIVATION OF COULOMB POTENTIAL ENERGY BETWEEN THE DISCRETE LAYERS

In this appendix, we give a derivation of the potential energy for the repulsive Coulomb interaction between the discrete layers, as expressed in Eq. (14). The electrostatic potential distribution V formed by an infinite charged sheet immersed in the plasma is given by the Poisson's equation in one dimension:

$$\frac{d^2V}{dz^2} = -\frac{e(n_i - n_e)}{\epsilon_0}. \tag{A1}$$

In a steady-state situation, the density n_j of plasma particles is given by a Maxwell–Boltzmann distribution: $n_j = n_0 \exp(-eV/k_B T_j)$, where n_0 is the density far away from the charged sheet. In the region where $|eV/k_B T_j| \ll 1$, we can expand the exponential in a Taylor series so that the Poisson's equation is represented:

$$\frac{d^2V}{dz^2} \simeq -\frac{n_0 e^2}{\epsilon_0 k_B}\left(\frac{1}{T_i} + \frac{1}{T_e}\right)V = \frac{1}{\lambda_D^2}\,V. \tag{A2}$$

The general solution for such a differential equation is well known as the following equation:

$$V = V_0 \exp\left(-\frac{|z|}{\lambda_D}\right), \tag{A3}$$

where V_0 is the potential on the charged sheet: $z=0$. Here V_0 is determined by the boundary condition for the electrostatic field E_0 on the charged sheet. Also, E_0 is obtained by Gauss' law by $E_0 = Q_d\sigma/2\varepsilon_0$. So, V_0 is given by a connection with Eq. (A3),

$$V_0 = \frac{\lambda_D \sigma Q_d}{2\epsilon_0}. \tag{A4}$$

Therefore, the potential energy W for the repulsive Coulomb interaction between the two charged sheets with a gap of z_{ij} per unit of area is eventually derived as the following equation:

$$W = \frac{1}{2}\,\sigma Q_d V = \frac{\lambda_D \sigma^2 Q_d^2}{4\epsilon_0} \exp\left(-\frac{z_{ij}}{\lambda_D}\right). \tag{A5}$$

Here, we note that W depends strongly on λ_D, and it may diverge with an extreme increase of λ_D. In the case of many sheets in the plasma, the potential energy for a repulsive Coulomb interaction between layers is given by summing them for all layers.

[1] H. Thomas, G. E. Morfill, V. Demmel, J. Goree, B. Feuerbacher, and D. Mohlmann, Phys. Rev. Lett. **73**, 652 (1994).
[2] J. H. Chu and I. Lin, Phys. Rev. Lett. **72**, 4009 (1994).
[3] Y. Hayashi and K. Tachibana, Jpn. J. Appl. Phys. **33**, L804 (1994).
[4] A. Melzer, T. Trottenberg, and A. Piel, Phys. Lett. A **191**, 301 (1994).
[5] J. B. Pieper, J. Goree, and R. A. Quinn, Phys. Rev. E **54**, 5636 (1996).
[6] H. Ikezi, Phys. Fluids **29**, 1765 (1986).
[7] H. Totsuji, T. Kishimoto, Y. Inoue, C. Totsuji, and S. Nara, Phys. Lett. A **221**, 215 (1996).
[8] H. Totsuji, T. Kishimoto, and C. Totsuji, Phys. Rev. Lett. **78**, 3113 (1997).
[9] V. E. Fortov, A. P. Nefedova, V. M. Torchinskii, V. I. Molotkov, A. G. Khrapak, O. F. Petrov, and K. F. Volykhin, JETP Lett. **64**, 92 (1996).
[10] S. Nunomura, N. Ohno, and S. Takamura, Jpn. J. Appl. Phys. **36**, L949 (1997).
[11] R. H. Norton, J. E. Guinn, W. C. Livingston, G. A. Newkirk, and H. Zirin, J. Geophys. Res. **72**, 815 (1967).
[12] A. B. Severny, E. I. Terez, and A. M. Zvereva, Space Res. **14**, 603 (1974).
[13] T. Nitter and O. Havnes, Earth, Moon, Planets **56**, 7 (1992).
[14] T. Nitter, Plasma Sources Sci. Technol. **5**, 93 (1996).
[15] W. L. Slattery, G. D. Doolen, and H. E. De Witt, Phys. Rev. A **21**, 2087 (1980).
[16] S. Ichimaru, Rev. Mod. Phys. **54**, 1017 (1982).
[17] D. Bohm and E. P. Gross, Phys. Rev. **75**, 1851 (1949).
[18] B. N. Chapman, *Glow Discharge Processes* (Wiley, New York, 1980), p. 109.
[19] J. G. Laframboise and L. W. Parker, Phys. Fluids **16**, 629 (1973).
[20] O. Havens, C. K. Goertz, G. E. Morfill, E. Grun, and W. Ip, J. Geophys. Res. **92**, 2281 (1987).
[21] M. S. Barnes, J. H. Keller, J. C. Forster, J. A. O'Neill, and D. K. Coultas, Phys. Rev. Lett. **68**, 313 (1992).
[22] G. E. Morfill and H. Thomas, J. Vac. Sci. Technol. A **14**, 490 (1996).